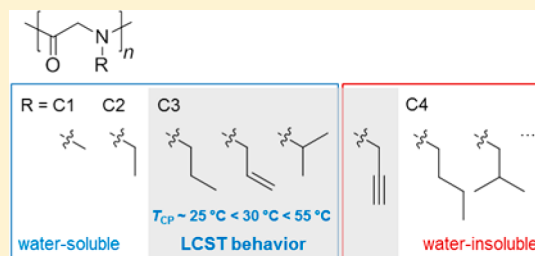


Thermoresponsive Poly(*N*-C3 glycine)sJoshua W. Robinson,<sup>†,‡</sup> Christian Secker,<sup>†,‡</sup> Steffen Weidner,<sup>§</sup> and Helmut Schlaad<sup>†,\*</sup><sup>†</sup>Department of Colloid Chemistry, Max Planck Institute of Colloids and Interfaces, Research Campus Golm, 14424 Potsdam, Germany<sup>§</sup>1.3 Structure Analysis, Federal Institute for Material Research and Testing (BAM), Richard-Willstätter-Strasse 11, 12489 Berlin, Germany

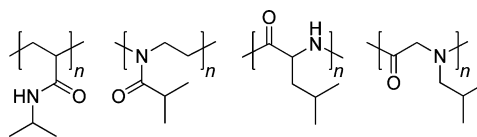
**ABSTRACT:** Ring-opening polymerization of *N*-substituted glycine *N*-carboxyanhydrides (NCAs) was applied to prepare a series of well-defined poly(*N*-C3 glycine)s (C3 = *n*-propyl, allyl, propargyl, and isopropyl), polypeptoids, with molecular weights in the range of 1.8–6.6 kg mol<sup>-1</sup>. Poly(*N*-isopropyl glycine), a previously unreported polypeptoid, could be obtained by bulk polymerization of the corresponding NCA in the melt. The samples were characterized by spectroscopy (NMR and FT-IR), size exclusion chromatography (SEC), and matrix-assisted laser desorption/ionization time-of-flight mass spectroscopy (MALDI–ToF MS). The polymers could be dispersed in water up to 20–40 g L<sup>-1</sup>; the poly(*N*-propargyl glycine) was not soluble in water. Turbidity measurements of the three water-soluble polypeptoids illustrated cloud point temperatures dependent on structural and electronic properties of the side chain. The cloud point temperatures were found to increase in the order C3 = *n*-propyl (15–25 °C) < allyl (27–54 °C) < isopropyl (47–58 °C). Long-term annealing of the aqueous solution of poly(*N*-{*n*-propyl} glycine) and poly(*N*-allyl glycine) above the cloud point temperature resulted in the formation of crystalline microparticles with melting points of 188–198 and 157–165 °C (differential scanning calorimetry, DSC), respectively, and rose bud type morphology (scanning electron microscopy, SEM).



## INTRODUCTION

“Smart” polymeric materials that react to external stimuli (i.e., pH, temperature, light, magnetic and electric fields, etc.) have received much attention over the years because of their commercial utility (self-healing, shape memory, piezoelectric, etc.) and/or biomedical (drug delivery, biosensing, etc.) applications.<sup>1</sup> In addition, research with stimuli-responsive materials provides insight and understanding into how the macromolecular systems’ morphology, conformation, and/or mechanic properties are influenced by noncovalent interactions (e.g., van der Waals, hydrogen bonding, and columbic/electrostatic forces). Thermo-responsive polymers based on polyethers, -esters, and -amides have been extensively investigated toward the aforementioned biomedical applications.<sup>2–4</sup> In particular the polyacrylamides and poly(2-oxazoline)s have demonstrated phenomenal tunable and precision controlled thermally induced biphasic separations, under aqueous conditions, as homo/copolymers, colloidal constructs, and networks (i.e., hydrogels).<sup>5–10</sup> In particular, poly(*N*-isopropylacrylamide) (PNIPAM) and poly(2-isopropyl-2-oxazoline) (PIPOX),<sup>11,12</sup> structural or constitutional isomers of each other (see Chart 1), have lower critical solution temperatures (LCST; 32 and 36 °C, respectively) near the physiological temperature range. For the most part, these polyamides readily undergo dissolution upon cooling demonstrating reversibility. However, PIPOX undergoes an irreversible biphasic separation upon long-term annealing above the cloud point temperature via a crystallization process occurring within the 2-phase region.<sup>13–15</sup> Such crystallization phenom-

**Chart 1. Selected [C<sub>6</sub>H<sub>11</sub>NO] Structural Isomers: Poly(*N*-isopropylacrylamide), Poly(2-isopropyl-2-oxazoline), Poly(2-isopropyl-2-oxazoline), Poly(2-isopropyl-2-oxazoline), Poly(2-isopropyl-2-oxazoline), Poly(2-isopropyl-2-oxazoline) (Left to Right)**



enon in solution has been observed for poly(2-oxazoline)s, yet for no other polymer.<sup>16</sup>

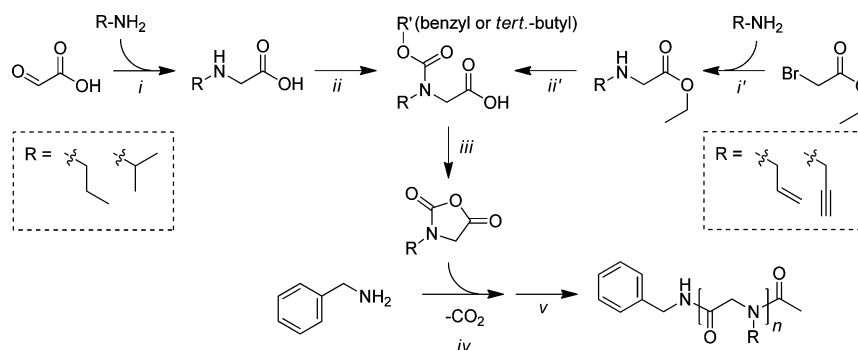
The thermo-responsive polymers PNIPAM and PIPOX (Chart 1) are constitutional isomers with either 2° or 3° amide side chains. Other isomers are the peptide-based main-chain polyamides poly(2-isopropyl-2-oxazoline) (PIPOX, 2° amide) and poly(*N*-isobutyl glycine) (PNIBG, 3° amide), neither of which demonstrated solubility in water or LCST behavior.<sup>17,18</sup> Although the insolubility of PL can be accredited to hydrogen bonding,<sup>19</sup> the solubility of PNIBG on a purely hydrophobic/hydrophilic ratio argument should have been consistent with that of PIPOX. However, the placement of the 3° amide (hydrogen acceptor) may play a significant role in solubility on an availability argument (hydrophobic pocket). Luxenhofer et al.<sup>18</sup> described some solubility investigations that confirmed the water solubility of poly(*N*-alkyl glycine)s, also referred to as

Received: November 22, 2012

Revised: January 16, 2013

Published: January 31, 2013

**Scheme 1. Three-Step Synthesis (*i–iii*) and Ring-Opening Polymerization (*iv, v*: Quenching with Ac<sub>2</sub>O) of *N*-C3 Glycine NCA, C3 = *n*-Propyl, Allyl, Propargyl, and Isopropyl**



polypeptoids,<sup>20,21</sup> with methyl (= polysarcosine)<sup>22</sup> and ethyl side chains. Polypeptoids with C3 chains (*n*-propyl) had limited solubility and those with C4 chains (*n*- and isobutyl) were insoluble in water. Shortly after, Zhang et al.<sup>23</sup> reported the solubility and cloud point temperatures ( $T_{cp}$ ) of statistical copolymers of poly(*N*-{ethyl/*n*-butyl} glycine) in aqueous solutions. From these studies, we rationalized that the solubility and suspected thermo-responsive behavior of poly(*N*-C3 glycine)s (C3 = *n*-propyl and also isopropyl, allyl, and propargyl) warranted further investigations. Notably, to the best of our knowledge, the poly(*N*-isopropyl glycine) has not yet been reported. We envisioned comparable results, in regards to LCST behavior and crystallinity, as described for the poly(2-oxazoline)s. Furthermore, the unique steric and electronic variations of the side chains would provide additional insight into side-chain influences on the LCST behavior.

## EXPERIMENTAL SECTION

**Materials.** Unless otherwise stated, all reagents were purchased and used as is from commercial sources (Sigma-Aldrich, Acros, or Alfa Aesar). Anhydrous solvents (*N,N*-dimethylformamide (DMF), *N,N*-dimethylacetamide (DMA), *N*-methyl-2-pyrrolidone (NMP), and benzonitrile (PhCN)) were purchased in bottles with a septum over molecular sieves; dichloromethane and acetic anhydride (Ac<sub>2</sub>O) were distilled from calcium hydride, tetrahydrofuran (THF) from sodium. All other solvents (1,4-dioxane, ethyl acetate (EtOAc), methanol (MeOH), etc.) were used as is from their respective commercial sources. Freshly distilled solvents were stored over activated molecular sieves (3 Å; 3–5 mm beads) and sealed under argon (flowed through a calcium chloride drying tube). Thin layer chromatography (TLC; 0.2 mm silica gel with fluorescent indicator; Polygram SIL G/UV<sub>254</sub>) plates with visualizing agents (UV, iodine chamber, or KMnO<sub>4</sub> stain) were utilized to monitor intermediate steps. Flash chromatography techniques were utilized with nitrogen pressure to push eluent/sample mixture through silica gel (pore size 60 Å; Fluka). All laboratory equipment was cleaned and oven-dried prior to use. The reaction flasks, for polymerization, were prepared by flash drying with a heat gun and reduced pressure (0.012 mbar).

**Monomer Synthesis.** The *N*-carboxyanhydrides (NCAs) of the *N*-C3 glycines, C3 = *n*-propyl (G<sup>-</sup>-NCA), allyl (G<sup>=</sup>-NCA), propargyl (G<sup>≡</sup>-NCA), and isopropyl (G<sup>+</sup>-NCA), were synthesized in three steps, starting from glyoxylic acid or  $\alpha$ -bromo ethylacetate and C3-amine, as described elsewhere (Scheme 1).<sup>18,24</sup> Exemplary procedure for the *N*-isopropyl glycine NCA: (G<sup>+</sup>-NCA, 3-isopropylloxazolidine-2,5-dione): (i) Glyoxylic acid monohydrate (59.92 g, 0.651 mol) was dissolved in reagent grade CH<sub>2</sub>Cl<sub>2</sub> (1.3 L) and mixed with isopropylamine (23.2 mL, 0.271 mol). The reaction was allowed to stir for 24 h at room temperature, and then the volatile organics were removed by rotoevaporation under reduced pressure. The remaining intermediate material was dissolved and refluxed (~24 h) in a 1 M hydrochloric acid solution (1.3 L). The aqueous medium was removed by rotoevapora-

tion under reduced pressure and the crude material was purified by recrystallization techniques utilizing MeOH and Et<sub>2</sub>O. The resulting *N*-isopropylaminoacetic acid was collected as a white crystalline material (15.23 g, 0.130 mol, 48%) with a melting point of 198 °C. <sup>1</sup>H NMR (DMSO-*d*<sub>6</sub>, 400 MHz):  $\delta$  13.74 (br s, 1H), 9.10 (s, 2H), 3.82 (s, 2H), 3.34–3.25 (m, 1H), 1.23 (d,  $J = 6$  Hz, 6H). (ii) A suspension of 2-(isopropylamino)acetic acid hydrochloride (15.46 g, 0.132 mol) was prepared in toluene (182 mL) and cooled via an ice bath. Once cooled, a 1 M solution of NaOH (398 mL) was added and stirred for 15 min. Benzyl chloroformate (19.13 mL, 0.134 mol) was injected into the stirring reaction. After 4 h, stirring was halted to allow for phase separation. The aqueous layer was extracted from the organic layer and the pH was adjusted to 1–2 via concentrated HCl. The layers were then recombined and shaken in a separatory funnel. The organics were extracted in EtOAc (3  $\times$  300 mL) and subsequently dried over MgSO<sub>4</sub>. Once filtered, the organic layers were concentrated down, by reduced vacuum techniques, to yield *N*-carboxybenzyl(Cbz)-*N*-isopropylaminoacetic acid as a viscous yellow oil (31.51 g, 0.125 mol, 95%). <sup>1</sup>H NMR (CDCl<sub>3</sub>, 400 MHz):  $\delta$  9.18 (br s, 2H), 7.45–7.22 (m, ~10H), 5.18, 5.13 (ss, 2H + 2H), 4.60–4.43–4.27 (mm, 1H + 1H), 3.96, 3.90 (ss, 2H + 2H), 1.13 (d,  $J = 7$  Hz, 12H). GC–MS (MSD):  $R_t = 10.8$  min; (EI)  $m/z$  251.2 (M<sup>+</sup>, [C<sub>13</sub>H<sub>17</sub>NO<sub>4</sub>]<sup>+</sup> = 251.12), 116.1 (M<sup>+</sup> – Cbz, [C<sub>5</sub>H<sub>10</sub>NO<sub>2</sub>]<sup>+</sup> = 116.07), 91.1 (benzyl, [C<sub>7</sub>H<sub>7</sub>]<sup>+</sup> = 91.05), 43.1 (isopropyl, [C<sub>3</sub>H<sub>7</sub>]<sup>+</sup> = 43.05). (iii) *N*-Cbz-*N*-isopropylaminoacetic acid (18.73 g, 74  $\mu$ mol) in a 2-neck round-bottom flask, fitted with a water cooled condenser, under positive argon pressure. Acetyl chloride (10.74 mL, 0.152 mol) was injected into this stirring solution and the reaction was subsequently refluxed for 5 h. The volatile organics were removed via rotoevaporation techniques to afford a crude yellow oil. Fraction distillation, under vacuum (0.03 mbar) with a heated condenser (~50 °C), afforded a crystalline material with yellow discoloration. <sup>1</sup>H NMR analysis suggests that the byproduct, benzyl chloride, was present as an impurity. Removal of this impurity was achieved via a liquid-melt-extraction technique utilizing heptanes. *N*-isopropyl glycine NCA was collected as a white crystalline material (7.68 g, 53.3 mmol, 72%) with a melting point of 59 °C. <sup>1</sup>H NMR (CDCl<sub>3</sub>, 400 MHz):  $\delta$  4.34–4.22 (m, 1H), 4.03 (s, 2H), 1.26 (d,  $J = 6.8$  Hz, 6H). <sup>13</sup>C NMR (CDCl<sub>3</sub>, 100 MHz):  $\delta$  165.7, 151.2, 45.2, 44.7, 19.9. FT-IR (crystal):  $\tilde{\nu}_{max}$  2981, 2940, 2888, 1842, 1755, 1452, 1416, 1395, 1376, 1361, 1290, 1242, 1198, 1154, 1130, 1075, 966, 900, 876, 808, 750, 682, 620 cm<sup>-1</sup>. GC–MS (MSD):  $R_t = 12.7$  min; (EI)  $m/z$  143.1 (M<sup>+</sup>, [C<sub>6</sub>H<sub>9</sub>NO<sub>3</sub>]<sup>+</sup> = 143.05), 128.0 (M<sup>+</sup> – O + H, [C<sub>6</sub>H<sub>9</sub>NO<sub>2</sub>]<sup>2+</sup> + H = 128.07), 56.1 (M<sup>+</sup> – isopropyl – 2O, [C<sub>2</sub>H<sub>2</sub>NO]<sup>3+</sup> = 56.01), 43.1 (isopropyl, [C<sub>3</sub>H<sub>7</sub>]<sup>+</sup> = 43.05).

**Polymer Synthesis.** The majority of poly(*N*-C3 glycine)s, C3 = *n*-propyl (PG<sub>*n*</sub><sup>-</sup>), allyl (PG<sub>*n*</sub><sup>=</sup>), and propargyl (PG<sub>*n*</sub><sup>≡</sup>), were synthesized as described elsewhere.<sup>18</sup> Poly(*N*-isopropyl glycine)s (PG<sub>*n*</sub><sup>+</sup>) were prepared as follows (exemplary procedure for the PG<sub>*n*</sub><sup>+</sup>): G<sup>+</sup>-NCA was transferred into a flash dried Schlenk flask prepared under an argon atmosphere. The sealed reactor flask was heated in an oil bath to ~5–10 °C above the melting point of the NCA. Once the substance was completely melted, the initiator solution (1 M benzylamine/NMP;

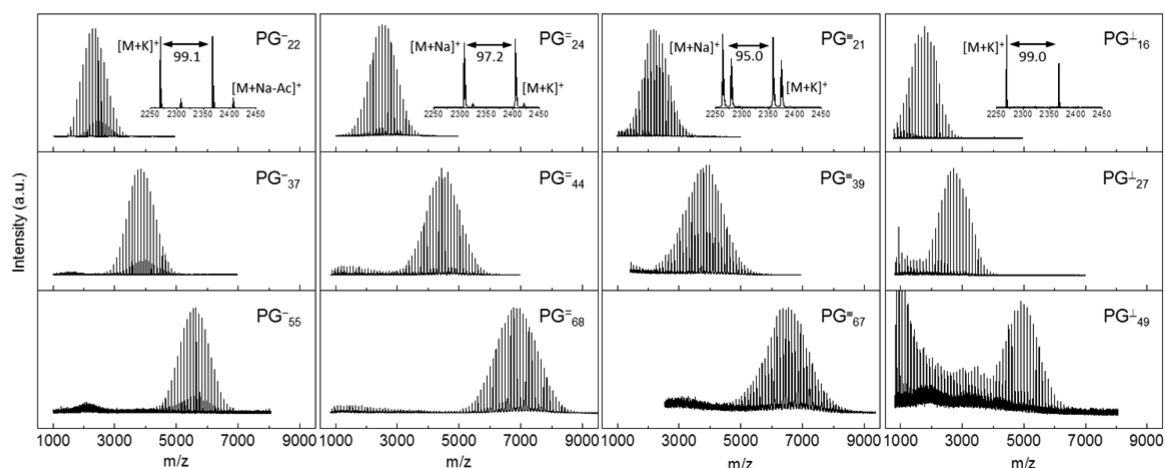


**Figure 1.** MALDI–ToF mass spectra of the series of synthesized poly(*N*-C3 glycine)s, C3 = *n*-propyl (PG<sup>−</sup><sub>*n*</sub>) (matrix/cation: DCTB/K<sup>+</sup>), allyl (PG<sup>=</sup><sub>*n*</sub>) (DCTB/Na<sup>+</sup>), propargyl (PG<sup>≡</sup><sub>*n*</sub>) (dithranol/Na<sup>+</sup>), and isopropyl (PG<sup>⊥</sup><sub>*n*</sub>) (DCTB/K<sup>+</sup>) (left to right).

[NCA]<sub>0</sub>/[BnNH<sub>2</sub>]<sub>0</sub> = 300) was injected into the reaction flask, and the mixture was heated to 160 °C. With time the oil became more viscous and around 2.5 h no further change was observed. The reaction was removed from the oil bath and cooled to room temperature. As crude <sup>1</sup>H NMR and GC–MS analysis detected unreacted monomer, the crude material was purified via dialysis (MWCO 500 Da, regenerated cellulose) against H<sub>2</sub>O (~3 d) then MeOH (~3 d). The remaining sample was concentrated down, via rotoevaporation under reduced pressure, to a slightly yellow material. <sup>1</sup>H NMR (DMF-*d*<sub>7</sub>, 600 MHz): δ 7.39–7.25 (m, 5H), 4.86–4.65 (br, ~59H), 4.61–3.91 (m, ~99H), 1.39–0.71 (m, ~292H). <sup>13</sup>C NMR (DMF-*d*<sub>7</sub>, 150 MHz): δ 170.8, 46.7, 44.9, 20.1; FT-IR (crystal)  $\bar{\nu}_{\max}$  2972, 2933, 2873, 1645, 1464, 1409, 1362, 1327, 1298, 1253, 1198, 1126, 1078, 996, 923, 846, 631, 589, 575 cm<sup>−1</sup>. MALDI–ToF–MS: *M*<sub>n</sub> = 5000 Da, Δ*m* = 99.2 ([C<sub>5</sub>H<sub>9</sub>NO] = 99.06 Da), residual mass, *r.m.* = 43.0. SEC (PS cal.): *M*<sub>n</sub><sup>app</sup> = 5430 g mol<sup>−1</sup>, *M*<sub>w</sub><sup>app</sup> = 7200 g mol<sup>−1</sup>, polydispersity index PDI = 1.26.

**Analytical Instrumentation and Methods.** Melting points were determined with a MEL-TEMP II apparatus, produced by Laboratory Devices Inc. (USA), in open capillaries. Gas chromatography–mass spectrometry (GC–MS): An Agilent Technologies GC 6890N MS 5975 equipped with an autosampler was utilized for analysis of compounds, purity, and detection of the monomer for polymerization monitoring. Samples were prepared in 2 mL septum-sealed vials at concentrations between 1–10 mg mL<sup>−1</sup>. Enhanced ChemStation software was utilized for the measuring program and analysis. Monomer measuring program: An aliquot of 1 μL was injected into the heating block (200 °C), split (50:50), and flowed (He; 0.757 bar) through the heated (50–200 °C; 2 min hold then 8 °C min<sup>−1</sup>) column. After a 2 min solvent delay, the data was captured (duration of 21.75 min) by the aforementioned software and subsequently analyzed. Nuclear magnetic resonance (NMR) spectroscopy: <sup>1</sup>H and <sup>13</sup>C NMR measurements were conducted on Bruker DPX-400 or Varian 600 MHz instruments at room temperature. Samples were prepared either in CDCl<sub>3</sub>, DMSO-*d*<sub>6</sub>, or DMF-*d*<sub>7</sub> (Aldrich) at concentrations of ~5–25 mg mL<sup>−1</sup>; signals were referenced to the signal of the solvent at δ <sup>1</sup>H 7.26 (<sup>13</sup>C 77.0), 2.50 (39.5), and 8.02 (162.6) ppm, respectively. Fourier transform infrared (FT-IR) spectroscopy: Measurements were completed on a Varian 1000 FT-IR, Scimitar series, equipped with an interchangeable sample head. Samples were loaded onto a diamond attenuated total reflectance (ATR) accessory and the Varian Resolutions FTS 1000 software allowed for measurements (transmittance; resolution =4; 32 scans) and the recording of data. Size exclusion chromatography (SEC): SEC with simultaneous UV (270 nm) and RI detection was performed in NMP (+0.5 wt % LiBr) at +70 °C, flow rate: 0.8 mL min<sup>−1</sup>, using a column set of two 300 × 8 mm<sup>2</sup> PSS-GRAM (spherical polyester particles with an average diameter of 7 μm) columns with porosities of

10<sup>2</sup> and 10<sup>3</sup> Å. Solutions containing ~0.15 wt % polymer were filtered through 0.45 μm filters; the injected volume was 100 μL. Calibration was done with polystyrene standards (Polymer Standards Service PSS, Mainz, Germany). The NTeqGPC V6.4 software (Wolfgang Schupp, Ober-Hilbersheim, Germany) was used for data recording and handling. Matrix-assisted laser desorption/ionization time-of-flight mass spectrometry (MALDI–ToF MS): Measurements were carried out with a Bruker Autoflex III Smartbeam MALDI (Bruker Daltonik), equipped with a laser working at 356 nm. Acceleration voltage was 20 kV and 4 × 500 shots at different places of the spot were recorded. Instrument software FlexControl and FlexAnalysis was used for data handling. Samples were prepared by applying the dried droplet method. 50 μL of matrix *trans*-2-[3-(4-*tert*-butylphenyl)-2-methyl-2-propenylidene]malononitrile, DCTB, or dithranol (10 mg mL<sup>−1</sup> in THF) were premixed with 20 μL of sample (2 mg mL<sup>−1</sup> in THF) and either sodium or potassium trifluoroacetate. One μL of that mixture was dropped on the target. Thermal analysis: Differential scanning calorimetry (DSC) was measured with a Mettler Toledo DSC1/TC100 at heating/cooling rates of 1 or 20 °C min<sup>−1</sup> under a nitrogen atmosphere. Glass transition temperatures were determined from second heating curves at 20 °C min<sup>−1</sup>. Thermogravimetric analysis (TGA) was carried out on a Netzsch TG 209 F1 at 20 °C min<sup>−1</sup> under a nitrogen atmosphere. Turbidity measurements were conducted on a T70+ UV–visible spectrometer fitted with a Peltier element (Tresser Instruments, Germany) operating at λ = 660 nm. The aqueous solutions in the cuvettes were heated/cooled at a rate of 1 °C min<sup>−1</sup> without stirring. The temperature at which the heating scan transmittance dropped to 80% was taken as the cloud point temperature. Scanning electron microscopy (SEM) images were taken with a Gemini Leo 1550 microscope operating at 3 kV. The samples were loaded on carbon-coated stubs and sputtered with Au/Pd 80/20 alloy prior to imaging.

## RESULTS AND DISCUSSION

**Synthesis.** The *N*-C3 glycine *N*-carboxyanhydrides (NCAs), C3 = *n*-propyl (G<sup>−</sup>-NCA), allyl (G<sup>=</sup>-NCA), propargyl (G<sup>≡</sup>-NCA), and isopropyl (G<sup>⊥</sup>-NCA), were synthesized in three steps as outlined in Scheme 1.<sup>18,24</sup> The ring-opening polymerizations of the NCAs, except G<sup>⊥</sup>-NCA (see below), were initiated with benzylamine ([NCA]<sub>0</sub>/[BnNH<sub>2</sub>]<sub>0</sub> = *n* = 25, 50, and 75) and conducted in dry benzonitrile solution (~10 wt %) for several days at room temperature.<sup>18</sup> For convenience, these polymerizations were carried out in Teflon sealable round-bottom flasks over the bench at reduced pressures.<sup>25</sup> A series of poly(*N*-C3 glycine)s PG<sup>−</sup><sub>*n*</sub>, PG<sup>=</sup><sub>*n*</sub>, and PG<sup>≡</sup><sub>*n*</sub> was isolated in high yields (>80%) and characterized by <sup>1</sup>H NMR and FT-IR spectroscopy, SEC (data not shown), and MALDI–ToF mass

**Table 1. Molecular Characteristics of the Poly(*N*-C3 glycine)s (*n*, Number-Average Degree of Polymerization;  $M_n$ , Number-Average Molecular Weight;  $M_n^{app}$ , Apparent Number-Average Molecular Weight; PDI, Apparent Polydispersity Index)**

sample	side chain R	end groups $\alpha/\omega$	NMR <sup>a</sup> <i>n</i>	MALDI–ToF MS <sup>b</sup>		SEC <sup>c</sup>	
				$M_n$ (kDa)	<i>n</i>	$M_n^{app}$ (kg mol <sup>-1</sup> )	PDI
PG <sup>-</sup> <sub>22</sub>	<i>n</i> -propyl	BnNH/Ac	22	2.37	22	2.5	1.16
PG <sup>-</sup> <sub>37</sub>	<i>n</i> -propyl	BnNH/Ac	37	3.85	37	4.1	1.19
PG <sup>-</sup> <sub>55</sub>	<i>n</i> -propyl	BnNH/Ac	55	5.64	55	6.2	1.19
PG <sup>=</sup> <sub>24</sub>	allyl	BnNH/Ac	21	2.63	24	3.8	1.05
PG <sup>=</sup> <sub>44</sub>	allyl	BnNH/Ac	35	4.51	44	6.9	1.04
PG <sup>=</sup> <sub>68</sub>	allyl	BnNH/Ac	45	6.63	68	10.1	1.03
PG <sup>≡</sup> <sub>21</sub>	propargyl	BnNH/Ac	21	2.07	21	3.1	1.05
PG <sup>≡</sup> <sub>39</sub>	propargyl	BnNH/Ac	37	3.80	39	5.4	1.04
PG <sup>≡</sup> <sub>67</sub>	propargyl	BnNH/Ac	51	6.46	67	9.9	1.04
PG <sup>⊥</sup> <sub>16</sub>	isopropyl	BnNH/Ac	17	1.78	16	2.7	1.53
PG <sup>⊥</sup> <sub>27</sub>	isopropyl	BnNH/H	27	2.81	27	3.9	1.14
PG <sup>⊥</sup> <sub>49</sub>	isopropyl	BnNH/H	50	5.00	49	5.4	1.26

<sup>a</sup><sup>1</sup>H NMR end group analysis,  $n = \text{integral}(-C(O)CH_2N-) \times 2.5 / \text{integral}(-C_6H_5)$ . <sup>b</sup> $n = (M_n - \text{BnNH} - (\text{Ac or H})) / \Delta m$ ,  $\Delta m$  = mass of repeat unit. <sup>c</sup>Apparent molecular weight distribution determined from the RI trace using a polystyrene calibration curve.

spectrometry (Figure 1) to confirm the chemical structures, as drawn in Scheme 1, and to access number-average molecular weights (degrees of polymerization) and molecular weight distributions (polydispersity indexes, PDI) – results are summarized in Table 1. Notably, there is excellent agreement between the number-average degrees of polymerization of PG<sup>-</sup><sub>*n*</sub> determined by <sup>1</sup>H NMR and MALDI–ToF MS, however, not so for PG<sup>=</sup><sub>*n*</sub> and PG<sup>≡</sup><sub>*n*</sub> (deviations are increasing with increasing chain length). The mass spectrometric results were taken as the absolute measure of *n*.

G<sup>⊥</sup>-NCA, on the other hand, could not (or very slowly) be polymerized under these conditions. Pioneering work by Ballard and Bamford support unfavorable kinetics (<10<sup>7</sup> dm<sup>3</sup> mol<sup>-1</sup> s<sup>-1</sup>) between isopropyl amine and G<sup>⊥</sup>-NCA.<sup>26</sup> Inference from this work suggested that the steric hindrance of the propagating species and the low concentrations of the monomer within a defined volume lower the statistical possibility of a favorable bimolecular reaction to occur (i.e., nucleophilic attack at the C5 position). Therefore, the increase in the concentration of monomer within a defined dimension should readily overcome the aforementioned limitation. In as much, polymerization occurred when the benzylamine was directly injected into the molten G<sup>⊥</sup>-NCA (mp 59 °C) ([NCA]<sub>0</sub>/[BnNH<sub>2</sub>]<sub>0</sub> = *n* = 25, 75, and 300) and then heated to 160 °C for 2.5 h. Reactions were optionally quenched with acetic anhydride and products purified by dialysis (see Experimental Section). The three PG<sup>⊥</sup><sub>*n*</sub> samples exhibited the expected chemical structures (<sup>1</sup>H NMR, FT-IR, MALDI–ToF MS) and degrees of polymerization of *n* ~ 17, 27, and 50 (<sup>1</sup>H NMR) (deviations from expected values are due to incomplete monomer conversions, estimated to be <40%). Although the poly(*N*-isopropyl glycine) chains underwent fragmentation during the MALDI–ToF mass spectrometric analysis (Figure 1, right), the experimental  $M_n$  values and calculated average degrees of polymerization (*n* ~ 16, 27, and 49) are in very good agreement with <sup>1</sup>H NMR results.<sup>27</sup> SEC analyses (data not shown) indicated monomodal and fairly narrow molecular weight distributions for PG<sup>⊥</sup><sub>27</sub> and PG<sup>⊥</sup><sub>49</sub>, but an apparently multimodal distribution for PG<sup>⊥</sup><sub>16</sub> (PDI ~ 1.5), which however is not observed by MALDI–ToF MS. Notably, SEC did not detect any low molecular weight or cyclic chains, thus excluding the occurrence of a self-initiated thermal polymerization of G<sup>⊥</sup>-

NCA (as it was observed by Kricheldorf et al. for sarcosine NCA in bulk at 120 °C).<sup>28</sup>

**Solubility and Thermal Properties.** The polymer samples, which were precipitated into petroleum ether, diethyl ether, or dialyzed against methanol and dried *in vacuo* at room temperature, with lowest molecular weights (*n* ~ 16–24) were subjected to first solubility tests in deionized water. PG<sup>-</sup><sub>22</sub> demonstrated limited solubility, as previously reported by Luxenhofer,<sup>18</sup> and also PG<sup>=</sup><sub>24</sub> and PG<sup>≡</sup><sub>21</sub> did not readily solvate in the aqueous environment. Just the PG<sup>⊥</sup><sub>16</sub> could be directly dissolved in water, up to 40 g L<sup>-1</sup> (PG<sup>⊥</sup><sub>*n*</sub> is soluble in water as well as in organic solvents like methanol, DMF, NMP, and chloroform). The solubility of PG<sup>-</sup><sub>22</sub> and PG<sup>=</sup><sub>24</sub>, but not PG<sup>≡</sup><sub>21</sub>, could subjectively be improved by changing the temperature of the medium, agitation, and various weight concentrations. Arguably, the variances in water solubility between the poly(*N*-C3 glycine) samples could not simply be explained by a hydrophilic/hydrophobic understanding. Instead we suspected that the difference could be due to (semi)crystallinity of the samples (see reports in the literature about the crystalline structures of peptoids<sup>29</sup> and related polyoxazolines<sup>13–16,30</sup>).

The thermal histories of the poly(*N*-C3 glycine)s were analyzed by DSC; the exemplary first heating curves at 1 °C min<sup>-1</sup> of PG<sup>-</sup><sub>37</sub>, PG<sup>=</sup><sub>44</sub>, PG<sup>≡</sup><sub>39</sub>, and PG<sup>⊥</sup><sub>27</sub> are shown in Figure 2 (gray lines). Endothermic melting transitions were observed for the samples PG<sup>-</sup><sub>37</sub> (two melting peaks at  $T_m = 190$ – $197$  °C) and PG<sup>=</sup><sub>44</sub> (one melting peak at  $T_m = 160$  °C), confirming their semicrystalline structures. PG<sup>-</sup><sub>37</sub> has a considerably higher crystallinity than PG<sup>=</sup><sub>44</sub>, as estimated from the respective melting enthalpies (areas under the endothermic peaks). Notably, no crystallization exotherm was revealed before melting of the PG<sup>-</sup><sub>37</sub>, suggesting that this sample was highly, if not fully, crystalline (see below). Melting transitions could not be detected for PG<sup>≡</sup><sub>39</sub> and PG<sup>⊥</sup><sub>27</sub>. Any melting transition of PG<sup>≡</sup><sub>39</sub>, however, could be buried under the strong exotherm observed at higher temperature,  $T > 150$  °C, which is attributed to a chemical reaction (not yet identified) followed by decomposition (sample turned red between 150–200 °C and into a black solid >200 °C without considerable mass loss until ~360 °C, TGA). PG<sup>⊥</sup><sub>27</sub> appears to be the only sample being completely amorphous. The glass transition temperatures of the polymers were determined from the second heating curves

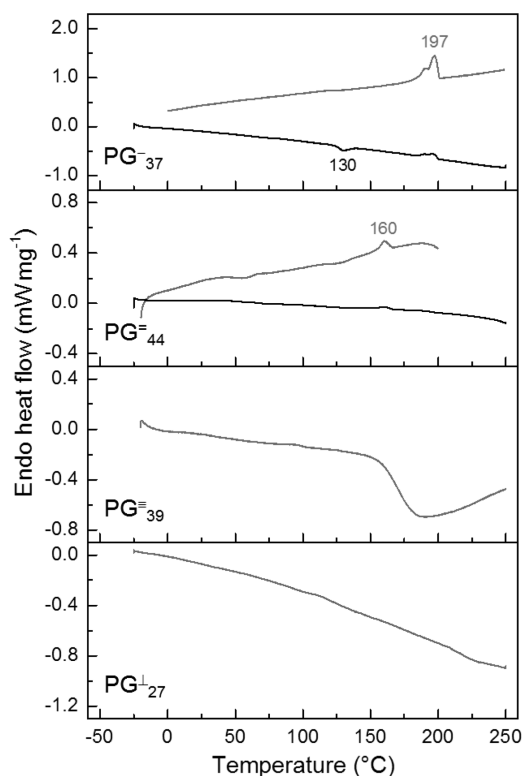


**Figure 2.** DSC first heating curves ( $1\text{ °C min}^{-1}$ ) of poly(*N*-C3 glycine)s, C3 = *n*-propyl ( $\text{PG}_{37}^{-}$ ), allyl ( $\text{PG}_{44}^{-}$ ), propargyl ( $\text{PG}_{39}^{\equiv}$ ), and isopropyl ( $\text{PG}_{27}^{\perp}$ ) as obtained after precipitation/dialysis and drying (gray lines) and after methanol treatment and drying *in vacuo* (black lines).

(data not shown) measured at  $20\text{ °C min}^{-1}$ :  $T_g \sim 64\text{ °C}$  ( $\text{PG}_{44}^{-}$ ),  $77\text{ °C}$  ( $\text{PG}_{37}^{-}$ ),  $108\text{ °C}$  ( $\text{PG}_{39}^{\equiv}$ ), and  $121\text{ °C}$  ( $\text{PG}_{27}^{\perp}$ ).

Attempting to remove crystalline domains,<sup>31</sup> the samples were dissolved in methanol (chosen for its hydrogen donating character and low boiling point,  $\sim 65\text{ °C}$ ) and subsequently the solvent removed under reduced pressure (complete removal of methanol confirmed by  $^1\text{H NMR}$ ). The DSC first heating curves of these methanol-treated samples are shown in Figure 2 (black lines). The endothermic melting peaks and crystallinities of  $\text{PG}_{37}^{-}$  and  $\text{PG}_{44}^{-}$  were found to be greatly reduced or completely erased (the exotherm at  $130\text{ °C}$  in the DSC scan of  $\text{PG}_{37}^{-}$  is attributable to crystallization of the sample,<sup>13</sup> not observed for  $\text{PG}_{44}^{-}$ ), whereas no structural change could be recognized for  $\text{PG}_{39}^{\equiv}$  (the sample is considered to be amorphous). The amorphous sample  $\text{PG}_{37}^{-}$  then demonstrated improved solubility in water, up to  $40\text{ g L}^{-1}$ , and the  $\text{PG}_{44}^{-}$  appeared to be soluble in water at low temperatures (plus time and agitation) and concentrations below  $20\text{ g L}^{-1}$ . The  $\text{PG}_{39}^{\equiv}$  was poorly soluble in methanol and unaffected by this treatment and remained insoluble in water. Acetone (bp  $\sim 56\text{ °C}$ ) and THF (bp  $\sim 66\text{ °C}$ ) were explored separately as alternative treatment techniques whereas  $0.1\text{ M NaOH}$  solutions were investigated as an alternative aqueous medium. None of these alternative treatments or conditions improved the solubility of  $\text{PG}_{39}^{\equiv}$  in aqueous media. In general, the solubility of the amorphous poly(*N*-C3 glycine)s in water decreased in the following order:  $\text{PG}_{27}^{\perp} \sim \text{PG}_{37}^{-} > \text{PG}_{39}^{\equiv} \gg \text{PG}_{44}^{-}$  (insoluble).

**Thermoresponsive Solution Behavior.** Here,  $0.1\text{--}1.0\text{ wt \%}$  ( $1\text{--}10\text{ g L}^{-1}$ ) aqueous solutions of  $\text{PG}_n^{-}$  ( $n = 22, 37$ , and

$55$ ),  $\text{PG}_n^{\equiv}$  ( $n = 24, 44$ , and  $68$ ), and  $\text{PG}_n^{\perp}$  ( $n = 16, 27$ , and  $49$ ) were prepared at room temperature or reduced temperatures ( $5\text{--}15\text{ °C}$ ). All sample solutions were visually confirmed to be optically clear prior to turbidity measurements. In addition, water was utilized as the zero reference (100% transmittance) for the UV-vis detector. The turbidity curves of the  $0.1$  and  $1.0\text{ wt \%}$  polymer solutions are presented in Figure 3. Also included in Figure 3 are the corresponding plots (phase diagrams) of the cloud point temperatures ( $T_{\text{CP}}$ ), determined as the temperature at which in the heating scan the transmittance dropped to  $\sim 80\%$ , versus the polymer concentration ( $0.1, 0.21, 0.34, 0.48$ , and  $1.0\text{ wt \%}$ ).

The phase transition appeared to be reversible for all solutions at concentrations below  $1.0\text{ wt \%}$ . Occasionally, translucent ribbons or white film/precipitates were observed in the lower 1/3 portion of the cuvette after the heating/cooling cycle. A change of concentration might affect the subsequent phase transition, possibly resulting in a shift of the solution clearing to a higher temperature than  $T_{\text{CP}}$  (as for instance recognized in the turbidity curve of  $\text{PG}_{22}^{-}$  at  $1.0\text{ wt \%}$ , Figure 3). Rather broad transitions, especially at low concentrations, and pronounced hysteresis between the heating and cooling scans ( $\Delta T \sim 3\text{--}10\text{ °C}$ ) were observed for the  $\text{PG}_n^{-}$  and  $\text{PG}_n^{\perp}$  solutions, whereas the  $\text{PG}_n^{\equiv}$  solutions revealed very sharp transitions with almost no hysteresis (similar to PNIAM).<sup>3</sup> Seemingly, the interchain association and dissociation process is delicately affected by the electronic properties of the side chain (unsaturation versus saturation) and less by the degree of branching. The allyl groups appear to be easier rehydrated than the propyl chains. Also worth to be considered are the possible different degrees of chain entanglement and the kinetics of *trans/cis* rotamerization of the  $3^{\circ}$  amide (as observed for PIPOX).<sup>15</sup>

The cloud point temperatures (not to be confused with the LCSTs) were found to be  $T_{\text{CP}} \sim 15\text{--}25\text{ °C}$  ( $\text{PG}_n^{-}$ ),  $27\text{--}54\text{ °C}$  ( $\text{PG}_n^{\equiv}$ ), and  $47\text{--}58\text{ °C}$  ( $\text{PG}_n^{\perp}$ ) (Figure 3, left). The  $T_{\text{CP}}$ s appeared relatively unaffected ( $\Delta T_{\text{CP}} \sim 5\text{ °C}$ ) by polymer concentration and chain length, at least in the examined experimental range, except those of  $\text{PG}_{22}^{-}$  and  $\text{PG}_{24}^{\equiv}$  solutions. The  $T_{\text{CP}}$ s of the  $\text{PG}_{24}^{\equiv}$  solutions were strongly increasing with decreasing concentrations and were shifted  $3\text{--}20\text{ °C}$  to higher temperature as compared to the solutions of the higher homologues ( $\text{PG}_{44}^{\equiv}$  and  $\text{PG}_{68}^{\equiv}$ ) (similar to PIPOX).<sup>3</sup> This behavior might be attributable to a better hydration of the shorter chains rather than to contributions of the end groups. The opposite, however unusual, trend was noticed for the  $\text{PG}_n^{-}$  series, the  $\text{PG}_{22}^{-}$  exhibiting the lowest  $T_{\text{CP}}$  of all samples (apart from  $\text{PG}_n^{\equiv}$ ). Similar observations (i.e., increasing  $T_{\text{CP}}$  with increasing degree of polymerization) were reported for dendronized polymer with peripheral oligo(ethylene oxide) chains<sup>32</sup> and poly(methoxy diethylene glycol acrylate)<sup>33</sup> and were explained by a tentatively poor shielding of short hydrophobic backbones from the water phase. Here, inversely, hydrocarbon chains are tethered to a polar polyglycine chain, which implies that the solvation is improved (i.e.  $T_{\text{CP}}$  is higher) when the backbone is less shielded. Accordingly, in respect to the  $T_{\text{CP}}$  values, the shielding of the backbone decreases in the order *n*-propyl  $>$  allyl  $>$  isopropyl, which seems to correlate with the rotational flexibility of the C3 chain. Notably,  $\text{PG}_n^{\equiv}$  is not or poorly soluble in water or methanol (see above), indicating that the polyglycine backbone is most efficiently shielded by propargyl groups. It is assumed that the solvation or hydration of the chains is hindered by favorable intrachain

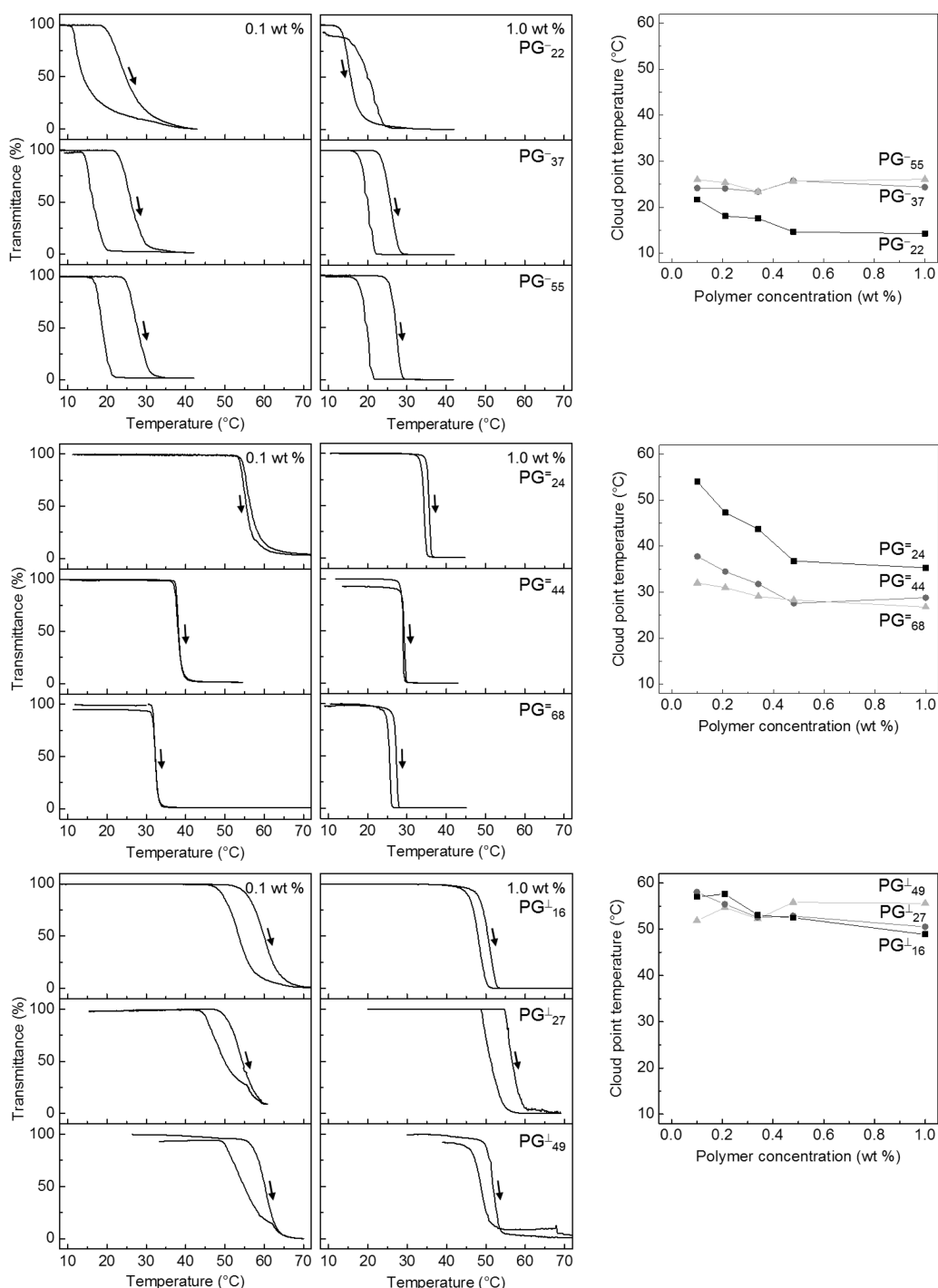


**Figure 3.** Turbidity curves (heating  $\rightarrow$  cooling at  $1\text{ }^{\circ}\text{C min}^{-1}$ ) of the 0.1 and 1.0 wt % aqueous solutions of poly(*N*-C3 glycine)s, C3 = *n*-propyl (PG<sup>-</sup><sub>*n*</sub>, *n* = 22, 37, and 55), allyl (PG<sup>=</sup><sub>*n*</sub>, *n* = 24, 44, and 68), and isopropyl (PG<sup>⊥</sup><sub>*n*</sub>, *n* = 16, 27, and 49) (left) and plots of the cloud point temperatures versus concentration (right).

coordination of the amide groups to the acetylene units through hydrogen bonding ( $\text{C}=\text{O}\cdots\text{H}-\text{C}\equiv\text{C}$ ) and/or  $n\rightarrow\pi^*$  interactions ( $\text{C}=\text{O}\cdots\text{C}\equiv\text{C}$ ).<sup>34,35</sup> For confirmation, the intra-chain interactions and also the polyglycine chain conformations need to be further analyzed, for instance by 2D-NMR and FT-IR/Raman spectroscopy.

**Crystallization in Solution.** Similar to PIPOX,<sup>14</sup> the possibility to produce crystalline particles by simple annealing of dilute aqueous polymer solutions at above the cloud point temperature was explored. Exemplarily, 0.5 wt % solutions of

PG<sup>-</sup><sub>37</sub> and PG<sup>=</sup><sub>44</sub> were annealed at  $75\text{ }^{\circ}\text{C}$  for 60 h and  $70\text{ }^{\circ}\text{C}$  for 24 h, respectively (annealing temperature was about 40 degrees above  $T_{\text{CP}}$ ). The formed precipitates were isolated by filtration, dried in vacuum for 12 h, and analyzed by DSC and SEM; the results are presented in Figure 4. The crystallized PG<sup>-</sup><sub>37</sub> was found to melt at  $188\text{--}198\text{ }^{\circ}\text{C}$  (two melting peaks), and particles were  $\sim 1\text{ }\mu\text{m}$  in diameter exhibiting a complex rose bud type morphology. The PG<sup>=</sup><sub>44</sub> particles, which melted at  $157\text{--}165\text{ }^{\circ}\text{C}$  (three melting peaks, possibly indicating the existence of different polymorphs), were considerably larger, measuring

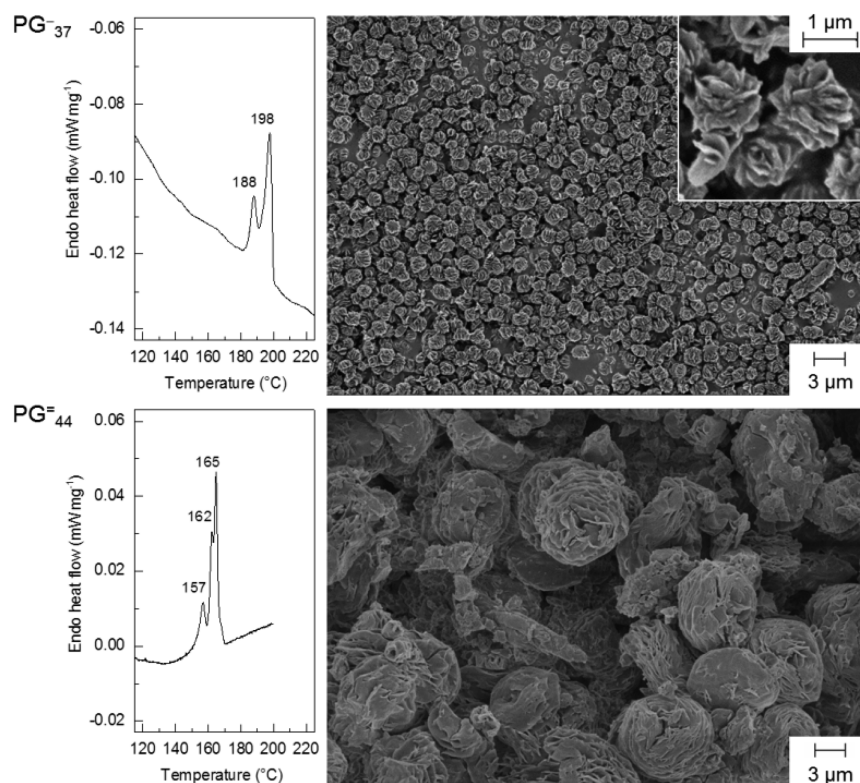


**Figure 4.** DSC first heating curves ( $1\text{ }^{\circ}\text{C min}^{-1}$ ) (left) and scanning electron micrographs (scale bar =  $3\text{ }\mu\text{m}$ , inset:  $1\text{ }\mu\text{m}$ ) (right) of the crystalline poly(*N*-C3 glycine)s  $\text{PG}_{37}^{-}$  and  $\text{PG}_{44}^{\equiv}$ , obtained by the annealing of 0.5 wt % aqueous polymer solutions at  $75\text{ }^{\circ}\text{C}$  (60 h) or  $70\text{ }^{\circ}\text{C}$  (24 h), respectively.

about  $10\text{ }\mu\text{m}$ , and less uniform in shape and size as compared to the  $\text{PG}_{37}^{-}$  particles. Seemingly, a slight variation at the side chain, saturated versus unsaturated, had severe impact on the phase separation (see above) and also on the morphology of the crystalline particles. Further details on the structures and crystallization kinetics/mechanism are not available yet.

## CONCLUSIONS

A series of polypeptoids based on *N*-C3 glycines ( $\text{C3} = n$ -propyl, allyl, propargyl, and isopropyl) with molecular weights of  $1.8\text{--}6.6\text{ kg mol}^{-1}$  was prepared by the ring-opening polymerization of the corresponding amino acid *N*-carboxyanhydrides. The poly(*N*-isopropyl glycine) ( $\text{PG}_n^{\perp}$ ), previously unreported, was obtained by the bulk polymerization in the melt. Initial attempts to dissolve the  $\text{PG}_n^{-}$  (*n*-propyl),  $\text{PG}_n^{\equiv}$  (allyl), and  $\text{PG}_n^{\equiv}$  (propargyl) in water were not successful, as supported by preliminary investigations completed by Luxenhofer et al.,<sup>18</sup> although the  $\text{PG}_n^{\perp}$  demonstrated solubility up to  $40\text{ g L}^{-1}$ . The insolubility of the  $\text{PG}_n^{-}$  and  $\text{PG}_n^{\equiv}$  series was caused by the semicrystallinity of the samples, which could be removed by treatment with methanol. Afterward the samples could be dissolved in water up to  $20\text{--}40\text{ g L}^{-1}$ . Overall, three out of the four poly(*N*-C3 glycine)s were soluble and demonstrated thermo-responsive behavior in water. The cloud point temperatures (reflecting the hydration of polymer chains) and the hysteresis (reflecting the interchain association and dissociation process) were delicately affected by the electronic and rotational flexibility of the side chains, less by the degree of branching. The C3 chains contribute to the shielding of the polyglycine backbone from the water phase, thus affecting the hydration of the polymer chain and the cloud point temperature. Accordingly, the cloud point temperatures

were found to increase in the order  $\text{PG}_n^{-}$  ( $T_{\text{CP}} \sim 15\text{--}25\text{ }^{\circ}\text{C}$ ) <  $\text{PG}_n^{\equiv}$  ( $27\text{--}54\text{ }^{\circ}\text{C}$ ) <  $\text{PG}_n^{\perp}$  ( $47\text{--}58\text{ }^{\circ}\text{C}$ ). Notably, the backbone was most efficiently shielded for  $\text{PG}_n^{\equiv}$ , rendering these samples insoluble in water, which might be attributable to intrachain interactions between the amide groups and the acetylene units (hydrogen bonding and/or  $n \rightarrow \pi^*$ -interactions). The sharpest phase transition and the least pronounced hysteresis were observed for  $\text{PG}_n^{\equiv}$ , which might be explained by a better hydration of unsaturated as compared to saturated side chains.

Similar to PIPOX, the  $\text{PG}_{37}^{-}$  and  $\text{PG}_{44}^{\equiv}$  underwent crystallization in 0.5 wt % aqueous solution upon long-term annealing at  $\sim 70\text{--}75\text{ }^{\circ}\text{C}$ , i.e. above the cloud point temperature. The formed precipitates were found to be crystalline microparticles with melting points of  $188\text{--}198$  and  $157\text{--}165\text{ }^{\circ}\text{C}$ , respectively, and rose bud type morphology.

These fundamental investigations provided significant insight into the thermo-responsive behavior and crystallization phenomena of polypeptoids with well-defined structures. However, further studies are required to address questions toward the influence that structural features and electronic properties appear to have on the solution behavior and crystallinity. A key to the better understanding of the system appears to be the conformation of the chains, which shall be analyzed in detail by NMR, FT-IR, and Raman spectroscopy. Also the kinetics and the mechanism of the polypeptoid crystallization in solution deserves further attention (X-ray scattering, calorimetry, and microscopy); results will be reported in due time.

Future studies will be devoted to use this polypeptoid platform for the preparation of smart (bio)functional micelles/vesicles, microparticles, and hydrogels for possible biomedical applications.

## AUTHOR INFORMATION

### Corresponding Author

\*E-mail: Helmut.Schlaad@mpikg.mpg.de (HS).

### Author Contributions

‡These authors contributed equally.

### Notes

The authors declare no competing financial interest.

## ACKNOWLEDGMENTS

Nora Fiedler, Jessica Brandt, Olaf Niemeyer, Marlies Gräwert, Rona Pitschke, and Heike Runge are thanked for their contributions to this work. Financial support was given by the Max Planck Society.

## REFERENCES

- (1) Cohen Stuart, M. A.; Huck, W. T. S.; Genzer, J.; Muller, M.; Ober, C.; Stamm, M.; Sukhorukov, G. B.; Szleifer, I.; Tsukruk, V. V.; Urban, M.; Winnik, F.; Zauscher, S.; Luzinov, I.; Minko, S. *Nat. Mater.* **2010**, *9*, 101–113.
- (2) Gil, E. S.; Hudson, S. M. *Prog. Polym. Sci.* **2004**, *29*, 1173–1222.
- (3) Dimitrov, I.; Trzebicka, B.; Müller, A. H. E.; Dworak, A.; Tsvetanov, C. B. *Prog. Polym. Sci.* **2007**, *32*, 1275–1343.
- (4) Aseyev, V.; Tenhu, H.; Winnik, F. *Adv. Polym. Sci.* **2011**, *242*, 29–89.
- (5) Hoogenboom, R. *Angew. Chem., Int. Ed.* **2009**, *48*, 7978–7994.
- (6) Schlaad, H.; Diehl, C.; Gress, A.; Meyer, M.; Demirel, A. L.; Nur, Y.; Bertin, A. *Macromol. Rapid Commun.* **2010**, *31*, 511–525.
- (7) Hoogenboom, R.; Schlaad, H. *Polymers* **2011**, *3*, 467–488.
- (8) Weber, C.; Hoogenboom, R.; Schubert, U. S. *Prog. Polym. Sci.* **2012**, *37*, 686–714.
- (9) Luxenhofer, R.; Han, Y.; Schulz, A.; Tong, J.; He, Z.; Kabanov, A. V.; Jordan, R. *Macromol. Rapid Commun.* **2012**, *33*, 1613–1631.
- (10) Kelly, A. M.; Wiesbrock, F. *Macromol. Rapid Commun.* **2012**, *33*, 1632–1647.
- (11) Park, J.-S.; Kataoka, K. *Macromolecules* **2006**, *39*, 6622–6630.
- (12) Huber, S.; Hutter, N.; Jordan, R. *Colloid Polym. Sci.* **2008**, *286*, 1653–1661.
- (13) Demirel, A. L.; Meyer, M.; Schlaad, H. *Angew. Chem., Int. Ed.* **2007**, *46*, 8622–8624.
- (14) Diehl, C.; Cernoch, P.; Zenke, I.; Runge, H.; Pitschke, R.; Hartmann, J.; Tiersch, B.; Schlaad, H. *Soft Matter* **2010**, *6*, 3784–3788.
- (15) Katsumoto, Y.; Tsuchiizu, A.; Qiu, X. P.; Winnik, F. M. *Macromolecules* **2012**, *45*, 3531–3541.
- (16) Diehl, C.; Dambowsky, I.; Hoogenboom, R.; Schlaad, H. *Macromol. Rapid Commun.* **2011**, *32*, 1753–1758.
- (17) Bellomo, E. G.; Wyrsta, M. D.; Pakstis, L.; Pochan, D. J.; Deming, T. J. *Nat. Mater.* **2004**, *3*, 244–247.
- (18) Fetsch, C.; Grossmann, A.; Holz, L.; Nawroth, J. F.; Luxenhofer, R. *Macromolecules* **2011**, *44*, 6746–6758.
- (19) Hanson, B.; Bedrov, D.; Magda, J. J.; Smith, G. D. *Eur. Polym. J.* **2010**, *46*, 2310–2320.
- (20) Kirshenbaum, K.; Barron, A. E.; Goldsmith, R. A.; Armand, P.; Bradley, E. K.; Truong, K. T. V.; Dill, K. A.; Cohen, F. E.; Zuckermann, R. N. *Proc. Natl. Acad. Sci. U. S. A.* **1998**, *95*, 4303–4308.
- (21) Zhang, D.; Lahasky, S. H.; Guo, L.; Lee, C.-U.; Lavan, M. *Macromolecules* **2012**, *45*, 5833–5841.
- (22) Gallot, B. *ACS Symp. Ser.* **1991**, *448*, 103–113.
- (23) Lahasky, S. H.; Hu, X.; Zhang, D. *ACS Macro Lett.* **2012**, *1*, 580–584.
- (24) Robinson, J. W.; Schlaad, H. *Chem. Commun.* **2012**, *48*, 7835–7837.
- (25) Habraken, G. J. M.; Wilsens, K.; Koning, C. E.; Heise, A. *Polym. Chem.* **2011**, *2*, 1322–1330.
- (26) Ballard, D. G. H.; Bamford, C. H. *J. Chem. Soc.* **1958**, 355–360.
- (27) Fetsch, C.; Luxenhofer, R. *Macromol. Rapid Commun.* **2012**, *33*, 1708–1713.

(28) Kricheldorf, H. R.; Lossow, C. V.; Lomadze, N.; Schwarz, G. J. *Polym. Sci., Part A: Polym. Chem.* **2008**, *46*, 4012–4020.

(29) Rosales, A. M.; Murnen, H. K.; Zuckermann, R. N.; Segalman, R. A. *Macromolecules* **2010**, *43*, 5627–5636.

(30) Litt, M.; Rahl, F.; Roldan, L. G. *J. Polym. Sci.: Part A-2* **1969**, *7*, 463–473.

(31) Diehl, C.; Schlaad, H. *Chem.—Eur. J.* **2009**, *15*, 11469–11472.

(32) Roeser, J.; Moingeon, F.; Heinrich, B.; Masson, P.; Arnaud-Neu, F.; Rawiso, M.; Mery, S. *Macromolecules* **2011**, *44*, 8925–8935.

(33) Miasnikova, A.; Laschewsky, A. *J. Polym. Sci., Polym. Chem.* **2012**, *50*, 3313–3323.

(34) Gorske, B. C.; Stringer, J. R.; Bastian, B. L.; Fowler, S. A.; Blackwell, H. E. *J. Am. Chem. Soc.* **2009**, *131*, 16555–16567.

(35) Caumes, C.; Roy, O.; Faure, S.; Taillefumier, C. *J. Am. Chem. Soc.* **2012**, *134*, 9553–9556.